A simulation model for the density of states and for incomplete ionization in crystalline silicon. I. Establishing the model in Si:P

P. P. Altermatt[a)]
Department Solar Energy, Institute Solid-State Physics, University of Hannover, Appelstrasse 2, 30167 Hannover, Germany

A. Schenk
Integrated Systems Laboratory, ETH Zurich, Gloriastrasse 35, 8092 Zurich, Switzerland and Synopsys Switzerland LLC, Affolternstrasse 52, CH-8050 Zürich, Switzerland

G. Heiser
School of Computer Science and Engineering, University of New South Wales, Sydney, New South Wales 2052, Australia

(Received 23 February 2006; accepted 21 August 2006; published online 8 December 2006)

A parametrization of the density of states (DOS) near the band edge of phosphorus-doped crystalline silicon is derived from photoluminescence and conductance measurements, using a recently developed theory of band gap narrowing. It is shown that the dopant band only "touches" the conduction band at the Mott (metal-insulator) transition and that it merges with the conduction band at considerably higher dopant densities. This resolves well-known contradictions between conclusions drawn from various measurement techniques. With the proposed DOS, incomplete ionization of phosphorus dopants is calculated and compared with measurements in the temperature range from 300 to 30 K. We conclude that (a) up to 25% of dopants are nonionized at room temperature near the Mott transition and (b) there exists no significant amount of incomplete ionization at dopant densities far above the Mott transition. In a forthcoming part II of this paper, equations of incomplete ionization will be derived that are suitable for implementation in device simulators. © *2006 American Institute of Physics*. [DOI: 10.1063/1.2386934]

I. INTRODUCTION

When the Fermi level E_F is situated close to the dopant level, the dopant states are noticeably occupied, leading to incomplete ionization (abbreviated as i.i.). The free carrier density is then noticeably smaller than the dopant density, although all dopant atoms replace Si atoms and are "electronically active." This statistical effect influences device behavior such as the current gain of transistors.

It is well known that i.i. is an important effect at low temperatures. However, it is commonly neglected in the simulation of silicon devices at room temperature. In this paper, it is demonstrated both theoretically and experimentally that there is up to 25% of i.i. at room temperature.

A few recent papers propose ways to implement i.i. in device models.[1–4] They conclude that there is an increasing amount of i.i. with increasing dopant density N_{dop}. However, we show here that these conclusions are incompatible with measurements: due to the metal-insulator transition, the dopant level approaches the band edge at high dopant densities, leading to rather complete ionization. Hence, i.i. is an important effect only in the N_{dop} range near 10^{18} cm^{-3}, as has been suggested decades ago.[5] In contrast to the above-mentioned papers, we carefully review and parametrize the dependence of the dopant level on N_{dop}, and additionally we consider broadening of the dopant states into a continuous band. Such a density of states (DOS) allows us to theoretically reproduce established measurements and to give an appropriate parametrization for i.i.

In this part I, a thorough physical basis for a DOS parametrization is given in phosphorus-doped crystalline silicon (Si:P) where the DOS is investigated most thoroughly (for an overview, see the most recent reviews on highly doped silicon[6–8]). This forms a firm base for the forthcoming part II of this paper, where the DOS parametrization will be expanded to other dopants in silicon and, finally, equations of i.i. will be derived that are suitable for implementation in device simulators to demonstrate some implications.

II. EXPERIMENTAL FOUNDATIONS FOR A DOS PARAMETRIZATION

In the following, a physical basis for the DOS parametrization is given. First, silicon at temperatures T below 10 K is considered, since the mechanisms determining the DOS have been mainly studied in this temperature range.

A. The DOS at low dopant densities

When a phosphorus atom replaces a Si atom in the crystal lattice, its outermost electron orbital has a ground state (*dopant state*) with an observed energy[9,10] $E_{\mathrm{dop},0}=-45.5$ meV below the conduction band edge E_c, and it is doubly[11,12] degenerate. There are also seven excited states observed below E_c, having various symmetries and hence various degeneracies.[9] However, most of these states are empty at

[a)]Electronic mail: altermatt@solar.uni-hannover.de

$T>20$ K where the parametrization will be applied, and therefore these states are neglected.[11] $E_{dop,0}$ cannot be calculated simply by using a hydrogenlike model (using the effective masses of conduction electrons and the dielectric constant $\epsilon=11.7$). This is so because the Coulomb attraction between the bound electron and its phosphorus core is screened by mobile electrons. Hence, $E_{dop,0}$ is sensitive to the type of dielectric screening, and the nonlinear Thomas-Fermi-Dirac screening theory reproduces the observed value of $E_{dop,0}$ with sufficient precision.[13] This type of screening depends only weakly on T,[13] so we regard $E_{dop,0}$ as independent of T in the parametrization.

In the following, we consider the properties of the dopant states with rising dopant density N_{dop}. We assume that the phosphorus atoms are randomly distributed in space because this very closely approximates reality.[14–16] At $N_{dop}<1\times10^{16}$ cm^{-3}, most neighboring phosphorus atoms are situated far apart, and their bound electrons do not interact with each other.[17] Thus, practically all dopant states have the same energy, leading to a peak in the far-infrared absorption spectrum that is as narrow[18] as 4.2 μeV (and is mainly broadened by isotopic randomness present in natural Si and, to a lesser extent, by lifetime broadening[18]). However, when two phosphorus atoms are randomly situated more closely together than two Bohr radii,[19] their dopant states undergo quantum mechanical mixing due to Coulomb interaction. At $N_{dop}>2\times10^{16}$ cm^{-3}, the number of such randomly occurring phosphorus pairs is large enough to cause the DOS of the dopant states to slightly broaden into a *dopant band* $D_{dop}(E)$. For example, its width is 2 meV at $N_{dop}=1.4\times10^{17}$ cm^{-3}.[17]

The higher the N_{dop}, the more phosphorus atoms are randomly situated closer together than two Bohr radii. Eventually, not only pairs are formed but also groups of various sizes,[17,19–22] called *dopant clusters*. At $N_{dop}>1\times10^{18}$ cm^{-3}, clusters containing three and four phosphorus atoms become more abundant than isolated phosphorus atoms.[20] This has two main effects. Firstly, the DOS broadens significantly,[17] because the dopant states within these clusters interact with each other. Secondly, E_{dop} starts to approach the conduction band edge, because the electrons are less strongly bound to the phosphorus cores with growing cluster size. Reference 20 gives a detailed microscopic insight into such clusters.

At 4.2 K, the electrons move rather freely within their clusters, as is concluded from magnetic susceptibility[23–26] and thermal conductivity[27–29] measurements. However, these electrons do not contribute to a macroscopic dc conductivity σ, since they cannot move from cluster to cluster within the dopant band. To contribute to σ, they need to be thermally excited to the conduction band; hence, σ is practically zero at low temperatures.[30–32] Only when N_{dop} reaches the critical value[30] of $N_{crit}=3.74\times10^{18}$ cm^{-3} can a sufficient number of clusters connect with each other so that the electrons can move freely, enabling a dc conductivity on a macroscopic scale. This prevents σ from dropping towards zero when the samples are cooled towards 0 K. The transition in the behavior of σ happens within a very small range of N_{dop} and is called the Mott, metal-insulator (M-I), or the metal-nonmetal (MNM) transition. The latter name originates from the observation that σ of metals does not drop near 0 K, while σ of insulators does.

We would like to mention that the above value of N_{crit} was determined using a commonly accepted procedure: by measuring σ at room temperature and by using the σ-N_{dop} relationship of Mousty *et al.*[33] These authors revised and extended the widely used σ-N_{dop} relationship of Thurber *et al.*[34] towards high N_{dop}. With the latter relationship, $N_{crit}=3.2\times10^{18}$ cm^{-3} would be obtained.

B. Does the M-I transition occur within the dopant band?

Above, we assumed that the clusters fuse on a macroscopic scale—while the dopant band is separate from the conduction band.[35] However, it is possible that the change in conductivity σ occurs simply because E_{dop} reaches the conduction band edge—while the clusters stay clearly separated from each other. In both cases, a metallic σ behavior is observed at low T. This means that more information than σ is needed to determine the causes of the M-I transition.

Indeed, it is widely accepted in the silicon community and written in textbooks that the dopant band merges with the conduction band at N_{crit}. This interpretation is based on photoconductivity,[36] infrared absorption,[37,38] and dielectric[39] measurements. However, this contradicts a second group of measurements, namely, magnetic resonance,[40] infrared reflectance,[41] and specific heat[24] measurements, which indicate that the M-I transition occurs within the dopant band while this band is still clearly separated from the conduction band. We solve the contradictions between these two groups of experiments with the following arguments.

(1) In the first group of measurements, the excitation of electrons to the conduction band is monitored. We show in Appendix A that from such measurements, E_{dop} was extracted incorrectly because the broadening of the dopant band was neglected. Instead, the activation energy[42] E_{act} was determined, which is the energy necessary to lift the most energetic electrons in the dopant band to the bottom of the conduction band, as depicted in Fig. 1(a).
(2) Hence, the above measurements indicate that, at N_{crit}, there is $E_{act}=0$ and there may be $E_{dop}\neq0$, i.e., the dopant band only "touches" the conduction band (instead of merging with it) when the clusters fuse on a macroscopic scale.

To give further independent evidence of $E_{act}=0$ and $E_{dop}\neq0$ at N_{crit}, we reinterpret the photoluminescence (PL) data of Bergersen *et al.*[43,44] These authors measured the PL spectrum of Si:P at various excitation powers at 4.2 K. At low powers, the PL spectrum shows the dopant band, because radiation is mainly caused by electrons that recombine from the dopant to the valence band. At high powers, the PL spectrum is dominated by electrons that recombine from the conduction band.[45]

In order to extract E_{dop} and E_{act} from the PL measurements, the electron energy E needs to be related to the detected photon energy E_{phot}. We take into account that Berg-

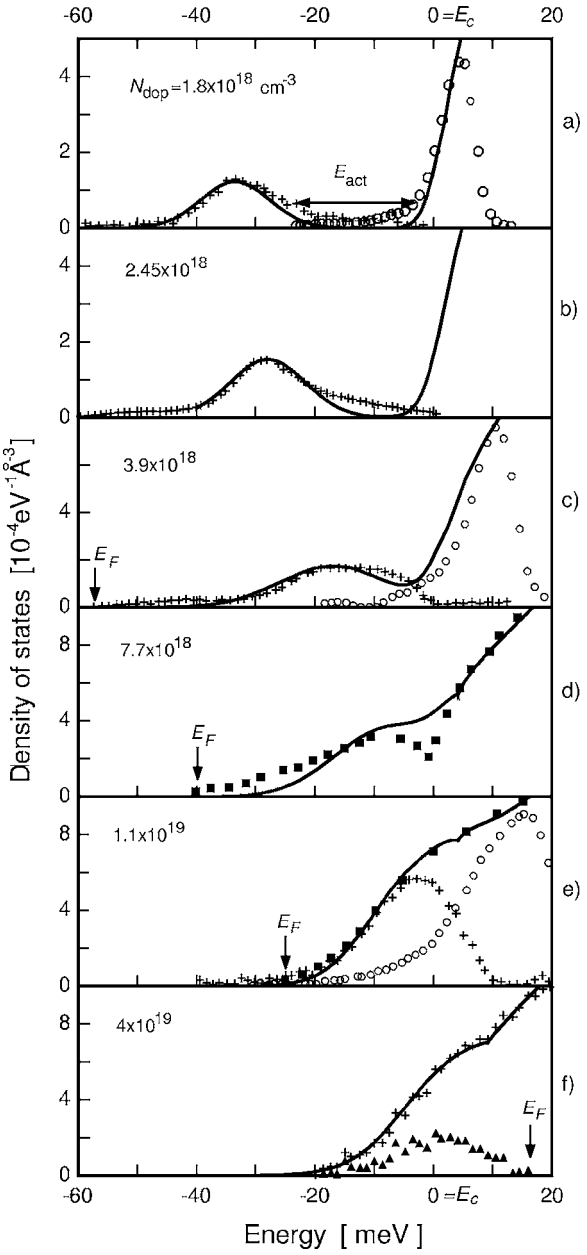

FIG. 1. The measured Si photoluminescence intensity (Refs. 43 and 44) (arbitrary units) at low injection power (crosses) and at high injection power (open circles), and the DOS derived from conductance measurements (Refs. 64 and 70) (squares), at various phosphorus densities and at 4.2 K. The solid lines are our parametrization of the DOS, Eqs. (2)–(9). The triangles in (f) are the difference between Eq. (2) and the crosses. The low injection signal has been scaled so that its integral equals bN_{dop}.

ersen *et al.* published the strongest PL peak that involves the emission of a transverse-optical (TO) phonon[46] with an energy of E_{phon}=58 meV,[47] and we use the equation

$$E = E_{phot} - E_g + \Delta E_g + E_{phon}, \quad (1)$$

where we scale E=0 at the conduction band edge E_c. E_g is the energy of the intrinsic band gap, which we compute with the analytical formula of Pässler.[48] With increasing power, a growing number of free carriers are injected into the sample, causing an increasing amount of band gap narrowing ΔE_g. In contrast to Bergersen *et al.*, we are able to calculate ΔE_g at both levels of excitation power, using the model of Ref. 49.[50] In the case of high powers, we use the hole density determined by Bergersen *et al.*

Our reevaluation of the PL data is shown in Fig. 1. The low (or high) excitation peaks are depicted as crosses (or open circles). At low excitation powers, the shape of the PL peak is directly proportional to the DOS of the dopant band. This is so because few holes are generated, and hence they are restricted to a very narrow energy range, which is kT =0.36 meV.[51] At 4.2 K, various interaction processes[52,53] broaden the peak additionally, but less than 1 meV. Also E_{phon} is broadened[54] and shifted[55,56] to less than 0.2 meV. The exciton density is too small to cause significant overlaps with the relevant peaks.[57]

At high excitation powers, the holes are distributed over a much broader energy range than at low powers. Thus, the PL line shape is a convolution of both the conduction and valence bands.

Figure 1(c) shows one of the important outcomes of this paper: the dopant band *just* touches the conduction band at N_{crit}. Is this an arbitrary coincidence? No for the following reasons. The theory of the ideal electron gas predicts that entirely free carriers have a parabolic energy-momentum (E-k) relation and hence a DOS $D_c \sim E^{1/2}$. Bound electrons have a flat E-k relation, which is curved more and more with a decreasing amount of localization;[58] this causes D_{dop} to widen with increasing N_{dop}. The electrons that become free on a macroscopic scale at N_{crit} do not contribute to the Gaussian D_{dop}; they are contained in the conduction band and make the transition when parts of D_{dop} exceed E=0, i.e., when D_{dop} touches the conduction band.

C. The DOS above the M-I transition

It is apparent from Fig. 1 that E_{dop} approaches the conduction band edge only gradually at dopant densities above N_{crit}. This is expected from theoretical investigations[20] showing that the dopant clusters have various sizes. Above N_{crit}, mainly small clusters remain isolated from the other clusters, and their electrons are rather strongly bound to the phosphorus cores, leading to $E_{dop} < E_c$. Galvanometric measurements[59] were also interpreted with a gradual merging of the dopant and conduction bands above N_{crit}.

To derive a parametrization of the DOS, the knowledge of E_{dop} alone is insufficient; it must be estimated which fraction b of the electrons is still bound to these isolated clusters. We should keep in mind that D_{dop} in Fig. 1 contains only the electron states bound to clusters, and not the free ones. With growing N_{dop}, there are fewer and fewer isolated clusters, causing more and more electrons to become free. A lower limit of b can be obtained from magnetic susceptibility and specific heat measurements.[24,28,60] From them, the density of electrons having localized magnetic momentum n_{lm} can be derived. The ratio n_{lm}/N_{dop} is depicted in Fig. 2 as crosses. This is only a lower limit for the following reasons.

(a) Only localized states with an odd occupation number carry a local magnetic moment.[23] To compensate for this, double the amount of n_{lm}/N_{dop} is plotted as filled symbols in Fig. 2 (hereby assuming a random distribution between odd and even occupation numbers).

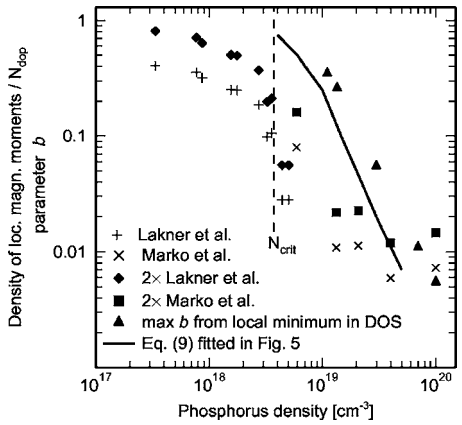

FIG. 2. The density of localized magnetic moments divided by N_{dop}, as derived from magnetic susceptibility and specific heat measurements (Refs. 24 and 28) (crosses). The twofold amount (squares) is a lower limit for the density of localized states in the dopant band. The upper limit is derived from DOS measurements (triangles). Parameter b (solid line) is adjusted by fitting the calculated amount of i.i. to experimental values.

(b) Many electrons in clusters have a sufficiently large localization length[61] such that their magnetic moment does not appear as localized. This is so because states near E_c are a hybridization of localized (quasiatomic) and extended states.[62,63] For these reasons, $n_{lm}/N_{dop} < 1$ below N_{crit}.

It becomes apparent from Fig. 2 that there exist a considerable number of localized electrons up to $N_{dop} \approx 1 \times 10^{19}$ cm^{-3}. This is so because physical parameters change relatively smoothly across the M-I transition if they depend on the internal structure of the clusters (such as the magnetic susceptibility and the specific heat coefficient). In contrast to this, other parameters change very abruptly at N_{crit} because they reflect how well the clusters are connected to each other (dc conductivity and dielectric susceptibility).

An upper limit to b can be obtained as follows. Depending on b, the overall DOS (of the dopant plus the conduction band) may or may not have a local minimum. For example, the DOS in Fig. 1(c) has a local minimum, while the DOS in Fig. 1(e) does not (unless b would be substantially increased). PL measurements are not feasible to confirm or deny such a local minimum because they are obtained using two different measurements at two different illumination intensities (crosses and open circles in Fig. 1). Fortunately, there are also DOS data available[64] that were derived[65–67] from current-voltage (I-V) measurements of n-Si/Sn tunnel structures. These measurements, shown in Fig. 1(d), confirm a local minimum in the overall DOS at −2 meV (even considering possible effects[68,69] caused by phonons). This is consistent with the observation[41] that, near this dopant density and at 10 K, electron transport occurs predominantly in the dopant band and not in the conduction band.

In such I-V measurements, a local minimum in the overall DOS causes a local minimum (V-type anomaly) in the dI/dV-V curve.[65] Such a minimum was also reported[70] up to 1×10^{19} cm^{-3} (for our reevaluation of some DOS data, see Appendix B). At $N_{dop} > 1 \times 10^{19}$ cm^{-3}, an anomaly occurring solely in the d^2I/dV^2-V curve was reported. In our interpretation, this so-called Λ-type anomaly occurs when the dopant band merges with the conduction band to the extent that the local minimum in the overall DOS disappears, but a "turning point" (between a convex and concave part of the DOS) remains. We will use these observations to find an upper limit of b in Sec. III D, where we calculate the overall DOS. The disappearance of the local minimum in the DOS and the appearance of a turning point agree with the interpretation of Knight shift measurements,[40,71] indicating that the dopant band merges completely with the conduction band at $N_{dop} \approx 2 \times 10^{19}$ cm^{-3}.

There is an additional reason why states are localized at $N_{dop} > 1 \times 10^{19}$. When the dopant band is merged with the conduction band, the DOS near the band edge is dominated by the band tail, which is mainly caused by disordering effects of dopants.[72] It is difficult to measure the DOS in the tail, because it is below the detection limit of PL measurements at low N_{dop}, while at high N_{dop} the PL peaks are broadened.[73,74] The tail DOS cannot be derived from tunneling measurements either, as such measurements are affected by interface states. This is why the dopant DOS in Fig. 1(d) extends artificially far into the band gap. For these reasons, it is necessary to derive the tail DOS from calculations alone, and we are going to do this in the section below.

Information about the DOS at still higher N_{dop} can be obtained by means of far-infrared reflectance spectra:[41] they can be accurately reproduced by the Drude model at $N_{dop} = 7.4 \times 10^{19}$ cm^{-3}, i.e., by assuming that the electrons are entirely free. This is also indicated by other transport properties, such as the magnetic field dependence[75] of the heat capacity,[76] nuclear magnetic resonance studies,[77] and Seebeck effect measurements.[78] The effective (density of states) electron mass m^*_{dc} used in these Drude calculations is essentially the same as at low dopant densities.[41] There are additional measurements[76,79,80] that indicate that m^*_{dc} depends only very weakly on N_{dop} up to $N_{dop} \approx 1 \times 10^{20}$ cm^{-3}. This implies that the DOS at such high dopant densities is essentially $\sim\sqrt{E}$ (apart from the band tail effects we are going to discuss in the next section).

III. PARAMETRIZATION OF THE DOS

So far, we have collected a thorough physical understanding of the DOS near the conduction band edge. Based on this, we now fit the DOS as precisely as possible to the values derived from experiments.

A. Calculation of the conduction band DOS and its tail state density

In order to arrive at a simulation model for i.i., the conduction band DOS needs to be calculated, including its tail states, with an approach[81] that stems from the following background. In the doping process, P atoms replace Si atoms, introducing bound states at the expense of band states (Levinson's theorem). The tail states arise when a sufficiently high number of Si atoms are replaced by P atoms such that the Si lattice becomes randomly disordered: locally attractive and repulsive potential fluctuations, respectively, lead to localized states that are below the conduction band

edge or above the valence band edge, respectively. These tail states also emerge at the expense of band states.[82] We use the envelope function proposed in Ref. 83 for computing the DOS of the conduction band. Its form is also justified by conductivity measurements near 0 K, which have been successfully interpreted using a superposition of the tail states and the dopant band.[84,85] The conduction band DOS is given by

$$D_k(E) = \frac{2N_c}{\sqrt{\pi}(kT)^{3/2}}\sqrt{\sigma_k}Y\left(\frac{E-E_c}{\sigma_k}\right), \tag{2}$$

where

$$\sigma_k = \frac{q^2}{\sqrt{4\pi\epsilon}}\sqrt{(N_D^+ + N_A^-)\lambda}\exp\left(-\frac{a}{2\lambda}\right) \tag{3}$$

and

$$Y(x) = \frac{1}{\sqrt{\pi}}\int_{-\infty}^{x}\exp(-u^2)\sqrt{x-u}du. \tag{4}$$

N_D^+ (N_A^-) is the density of ionized donors (acceptors), and $a = 0.543$ nm denotes the lattice constant of silicon,[86] which is constant up to very high N_{dop}.[87,88] The effective density N_c is calculated using Ref. 89. The Debye screening length λ is calculated using the Thomas-Fermi approximation:

$$1/\lambda^2 = \frac{4\pi q^2}{\epsilon}\frac{\partial n}{\partial E_{Fn}}. \tag{5}$$

Equation (5) is derived neglecting the dopant band, which has only negligible consequences for the simulation model.

B. Fitting of D_{dop}, E_{dop}, and E_{act}

Experiments[43,64,70] and calculations[20,43,58,62,63,90–97] indicate that the broadening of the dopant DOS is not necessarily symmetrical with respect to E_{dop}. However, Fig. 1 justifies that D_{dop} can be closely approximated by a Gaussian distribution function:

$$D_{\mathrm{dop}}(E,N_{\mathrm{dop}}) = \frac{N_{\mathrm{dop}}b}{\sqrt{2\pi}\delta}\exp\left[\frac{-(E-E_{\mathrm{dop}})^2}{2\delta^2}\right]. \tag{6}$$

Here, δ the half-width of the dopant DOS and b is the fraction of bound states.

We extract E_{dop} and E_{act} from Fig. 1 and compare these values in Fig. 3 with photoconductivity,[36] infrared absorption,[37,38] and dielectric[39] measurements, as described in Appendix A. Because D_{dop} can be closely approximated by a Gaussian (which means symmetrical) profile in Fig. 1, the difference between E_{dop} and E_{act} is approximately half the width of the dopant band, δ.

In Fig. 3, the data of Ref. 98 are omitted because they were derived from consistency arguments where i.i. was neglected. The data of Ref. 99 are not shown either, as they were obtained from compensated silicon; both experimental[100–103] and theoretical[62,104–106] studies indicate that compensation influences E_{dop} and E_{act} considerably. Accounting for all this, it follows that the E_{act} values in Fig. 3 coincide with the other experimental data within the experimental errors.

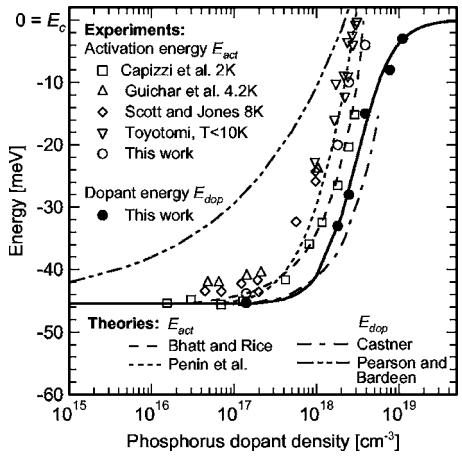

FIG. 3. The energy of the dopant band peak E_{dop} (filled circles) and the activation energy of the dopant band E_{act} (empty circles), as derived from Fig. 1. The other symbols show E_{act} values, obtained from various measurement techniques (Refs. 36, 37, 39, and 125). The solid line is the parametrization using Eq. (7). The dashed lines show theoretical computations (Refs. 5, 42, 99, and 107).

From Fig. 3 it becomes apparent that E_{act} starts to change at $N_{\mathrm{dop}} \approx 10^{17}$ cm^{-3} due to band broadening and that E_{dop} stays rather constant up to $N_{\mathrm{dop}} \approx 1\times10^{18}$ cm^{-3}, as also optical studies show.[17]

At higher N_{dop}, both parameters change rather abruptly. E_{act} becomes zero at the M-I transition, while E_{dop} approaches zero (i.e., E_c) gradually above $N_{\mathrm{dop}} \approx 1\times10^{19}$ cm^{-3}. E_{dop} cannot move into the conduction band because the principal reason for its variation is screening.

We parametrize the E_{dop} values with the logistical equation

$$E_{\mathrm{dop}} = \frac{E_{\mathrm{dop},0}}{1+(N_{\mathrm{dop}}/N_{\mathrm{ref}})^c}, \tag{7}$$

using the parameters listed in Table I. The results are shown as a solid line in Fig. 3.

The dependence of E_{dop} and E_{act} found here is similar to various calculations.[42,99,107] However, the early theory of Pearson and Bardeen[5] deviates significantly from more recent experimental data. This is an important result, as this early theory is commonly used to quantify E_{dop}.[108,109] In fact, Fig. 3 shows that most of the changes in E_{dop} and E_{act} occur near N_{crit}. This behavior was predicted in Refs. 110 and 111 where it is argued that E_{dop} is quite insensitive to doping at

TABLE I. The parameters used in Eqs. (6)–(9) and (11) to describe the density of states of the dopant band.

Parameter	Si:P
$E_{\mathrm{dop},0}$ (meV)	45.5
N_{ref} (cm^{-3})	3×10^{18}
c	2
r (eV cm$^{-3/2}$)	4.2×10^{-12}
s (cm^{-3})	10^{19}
N_b (cm^{-3})	6×10^{18}
d	2.3
g	1/2

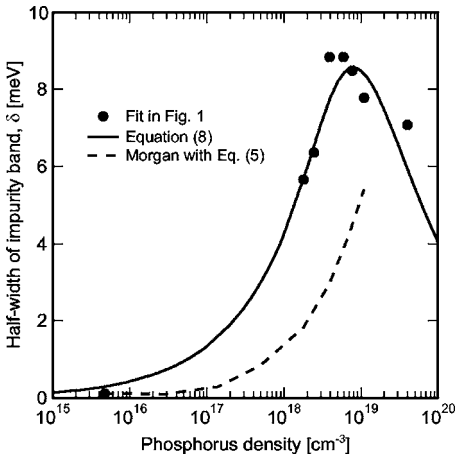

FIG. 4. The half-width of the dopant band (filled circles), defined by δ in Eq. (6), which empirically describes the experimental data in Fig. 1. The solid line is a parametrization given by Eq. (8). The dashed line is calculated by Morgan (Ref. 90) with the Thomas-Fermi screening theory, using Eq. (5).

$N_{dop} < 1 \times 10^{18}$ cm^{-3} because the dopant states are not effectively screened by the electrons in the conduction band.

C. Fitting of the bandwidth

We extract the half-width of the dopant band, δ, by fitting the PL measurements in Fig. 1 with Eq. (6). The results are shown in Fig. 4 as symbols. It is apparent that δ increases with increasing N_{dop} up to N_{crit} because the dopant clusters grow (see Sec. II A for a detailed explanation). With growing N_{dop} beyond N_{crit}, δ decreases because smaller and smaller clusters stay isolated and contribute to D_{dop}. We do not know how reliably we can extract δ from the data in Fig. 1. However, we will show below that variations in δ have only a minor influence on the effects caused by the DOS.

For an empirical expression of δ, we choose

$$\delta = rN_{dop}^{1/2}(1 - e^{-s/N_{dop}}), \tag{8}$$

using the parameters of Table I. The data fit is shown as solid line in Fig. 4.

The broadening of the dopant DOS was calculated by a number of authors.[20,43,58,62,63,90–97] The dashed line in Fig. 4 shows that Morgan's theory[90] underestimates the broadening of the dopant band if the Thomas-Fermi screening theory of Eq. (5) is used. The reason for this is the formation of clusters, which is not considered by Morgan. More elaborate theories that include clusters depend sensitively on the screening length within the clusters themselves—which, in turn, is not accessible to experiments and hence is not precisely known. We have therefore found it difficult to compare these theories with the PL data of Fig. 1.

It is important to mention that the Hubbard model[112] predicts a second dopant band situated near the conduction band edge.[113] This second band was forecast to be stable in silicon,[114] and it was detected in absorption, photoconductance, and magnetic susceptibility measurements.[25,115,116] As it contains 10^{13} cm^{-3} electrons at most,[115] we neglect it in the DOS parametrization.

D. Fitting of parameter *b*

The only remaining parameter to be fitted to experimental values is b, which quantifies the fraction of electrons that remains bound to dopant clusters above N_{crit}. In Sec. II C, a lower limit of b was obtained from magnetic susceptibility measurements. This limit is shown as squares in Fig. 2. We also discussed in Sec. II C that an upper limit of b can be obtained from DOS measurements because there is no local minimum of the DOS observed at high N_{dop}, implying that $b < 1$. We now determine this upper limit of b by calculating the DOS with Eqs. (2)–(8) such that no local minimum occurs at $N_{dop} \geqslant 1 \times 10^{19}$. The results are shown as triangles in Fig. 2. As it is an upper limit, it lies above the squares, except near $N_{dop} = 10^{20}$ cm^{-3}, where more localized magnetic momenta seem to arise due to band tailing than due to the dopant band.

These upper and lower limits generally lie far apart, and no precise adjustment of b is possible on these grounds. However, b strongly influences the amount of i.i. Therefore, we will adjust b in Sec. V by fitting the calculated i.i. to experimental values. We will assume that $b=1$ below N_{crit} and that

$$b = \frac{1}{1 + (N_{dop}/N_b)^d} \tag{9}$$

above N_{crit}.

IV. THE DOS OF THE DOPANT BAND ABOVE 10 K

So far, we based the parametrization on measurements that were obtained at temperatures below 10 K. We found it impossible to derive the DOS from PL measurements performed at temperatures far above 10 K for three reasons: firstly, the dopant peak disappears at the higher excitation intensities[43] used in most of the room temperature PL measurements;[117,118] secondly, even if low excitation intensities can be maintained, the peak disappears at $T \geqslant 49$ K;[119] and thirdly, the PL spectrum is affected by lifetime broadening at temperatures well above 10 K.[52] See Ref. 45 for a more detailed discussion of how the PL spectrum depends on temperature and excitation levels.

The disappearance of the dopant peak at higher temperatures is not well understood.[100,120,121] For example, it was proposed that the dopant band may merge with the conduction band at $T > 49$ K, because free electrons are thermally generated to the conduction band, where they contribute to screening more effectively than when staying localized in the dopant band.[45,119] However, no change in free carrier density near 49 K has been observed, which would occur if the dopant band disappeared. In addition, electron paramagnetic resonance studies[122] and Seebeck measurements[78] indicate that the dominant transport mechanism of electrons already changes at approximately 15 K from hopping/tunneling (in and from the dopant band) to transport within the conduction band.

We expect that E_{dop} is rather insensitive to temperature because the nonlinear Thomas-Fermi-Dirac screening theory reproduces very well the experimentally determined value of E_{dop} at low temperatures,[13] and this type of screening de-

pends only weakly on T. We expect that the width of the dopant band may broaden with rising temperature. Fortunately, the calculation of the free carrier density and i.i. depends only weakly on δ, as will be shown in the following section.

V. INCOMPLETE IONIZATION

In this section, the amount of i.i. is calculated with the above parametrization and verified with experimental data. Up to about 400 K, the free electron density n equals the ionized phosphorus density N_{dop}^{+}, so i.i. is the ratio $n/N_{\mathrm{dop}} = N_{\mathrm{dop}}^{+}/N_{\mathrm{dop}}$. The amount of i.i. is obtained by self-consistently solving the three following equations at a given N_{dop}:

$$N_{\mathrm{dop}}^{0} = \int_{-\infty}^{E_{\mathrm{mob}}} [D_{\mathrm{dop}}(E) + D_k(E)] f_D(E,E_F) dE, \tag{10a}$$

$$N_{\mathrm{dop}}^{+} = \int_{E_{\mathrm{mob}}}^{\infty} [D_{\mathrm{dop}}(E) + D_k(E)] f(E,E_F) dE, \tag{10b}$$

$$N_{\mathrm{dop}} = N_{\mathrm{dop}}^{0} + N_{\mathrm{dop}}^{+}, \tag{10c}$$

where N_{dop}^{0} is the neutral (nonionized) dopant density and E_{mob} is the energy above which the states host mobile carriers (large parts of the band tails host immobile carriers). The unknown parameters in this equation system are N_{dop}^{0}, N_{dop}^{+}, and E_F. The occupation probability of the dopant states,

$$f_D = 1/(1 + g e^{(E-E_{Fn})/kT}), \tag{11}$$

differs from the Fermi-Dirac function f by the degeneracy factor g, because each localized state in the dopant band can be occupied by only a single electron due to the Coulomb interaction, which prevents the occupation by two localized electrons with opposite spin. Also, such a state can be occupied by an electron in two ways (having spin up or spin down), while it can be empty in only one way, causing $g = 1/2$.[123,124] We need to keep in mind that some of the dopant states are locally free within dopant clusters,[24,28] and this may cause g to increase towards unity.

The only parameter in D_{dop} that is not fixed so far is b. In the following, b is fitted by comparing the calculations with experimental values of i.i.

How can measurements of n/N_{dop} be obtained? The amount of incomplete ionization can be extracted from the ratio between published[33,125–132] conductivity mobility $\mu_{\mathrm{cond}} = \sigma/qn$ and Hall mobility $\mu_H = \sigma R_H/r$. The former is almost always obtained by measuring the conductivity σ (via a four-point probe) and with the assumption that $n(N_{\mathrm{dop}},T) = N_{\mathrm{dop}}$, i.e., by neglecting i.i. N_{dop} is derived from the measured σ values and using a established $N_{\mathrm{dop}}-\sigma$ relationship. In order to obtain a consistent data set, we assign to every published σ value a N_{dop} value by using solely the $N_{\mathrm{dop}}-\sigma$ relationship of Mousty *et al.*[33]

The Hall mobility is derived from measurements of both σ and the Hall factor R_H. The Hall correction factor r is usually assumed to be unity, although it is well known that it depends on the dominant scattering mechanism and therefore on T and N_{dop}.[125,126,133] We take

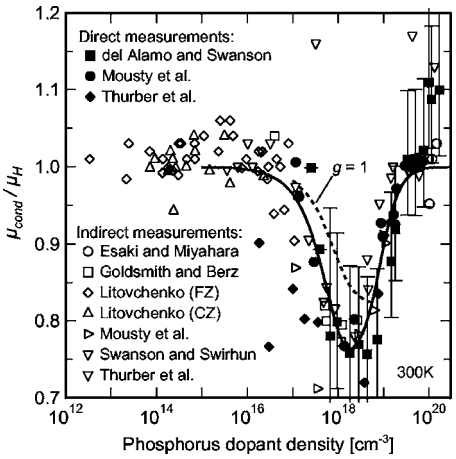

FIG. 5. The fraction between measured conductivity mobility and Hall mobility (symbols) (Refs. 33, 98, and 125–132), reflecting incomplete ionization, which is compared with parametrizations (lines).

$$r = 1.18 + \frac{0.18}{(1 + N_{\mathrm{dop}}/10^{17})^{0.8}} \tag{12}$$

from Ref. 134 at 300 K. Again, in order to obtain a consistent data set, we assign to every published σ value a N_{dop} value using solely the $N_{\mathrm{dop}}-\sigma$ relationship of Mousty *et al.*[33]

Plotted under these conditions, $\mu_{\mathrm{cond}}/\mu_H$ quantifies i.i., because i.i. is neglected in μ_{cond} but included in μ_H. A collection of literature values is shown in Fig. 5. The direct measurements[33,126,127] were obtained by measuring μ_H and μ_{cond} in the same samples. The indirect measurements[98,125,128–132] are μ_H measurements that we related to an empirical parametrization of μ_{cond}, as is explained in Ref. 134.

Our parametrization, using Eqs. (10a)–(10c), fits the experimental data very well within the experimental precision if we adjust b with Eq. (9), using the parameters of Table I. This implies that at the M-I transition, only about 5% of electrons in the clusters become free (see Fig. 2). We have not found any experimental verification of this in the literature.

The calculations with $g=1$ (instead of $g=1/2$) are shown as dashed line in Fig. 5 and underestimate i.i. below N_{crit}. This suggests that the dopant band contains mainly localized states, which is consistent with the magnetic susceptibility measurements shown in Fig. 2.

Our calculations and the experimental data in Fig. 5 are significantly different from various published models shown in Fig. 6. Li and Thurber[109] calculated E_{dop} using the pioneering theory of Pearson and Bardeen[5] (shown in Fig. 3) and obtained an amount of i.i. that is significantly lower than observed here. It is important to note that this influences the $N_{\mathrm{dop}}-\mu_{\mathrm{cond}}$ relationship of Thurber *et al.*[128] which has become a standard in the silicon community. We have corrected Thurber's mobility data by the updated amount of i.i. in a separate paper.[134] Kuzmicz[135] extended the theory of Li and Thurber; but his theory does not describe the experiment either. Moreover, the calculations that assume a constant E_{dop}, discussed in the Introduction, overestimate i.i. tremen-

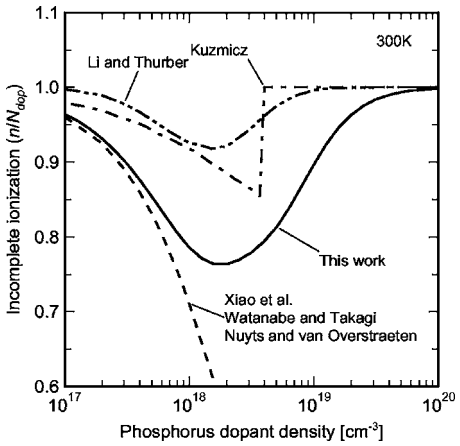

FIG. 6. The fraction of nonionized phosphorus atoms, calculated with Eqs. (10a)–(10c) (solid line). The theories of Li and Thurber (Ref. 109) and of Kuzmicz (Ref. 135) underestimate i.i., while theories assuming a constant E_{dop} overestimate it tremendously at $N_{dop}>10^{18}$ cm^{-3} (Refs. 1, 2, 4, and 136).

dously at $N_{dop}>10^{18}$ cm^{-3}.[1,2,4,136] The measurements in Fig. 5 clearly invalidate such large amounts of i.i.

One of the central results of this paper is that at 300 K, up to 25% of donors are nonionized—a result that challenges common beliefs that i.i. can be neglected at room temperature. Previous measurements of the μ_{cond}/μ_H ratio, such as Refs. [33,127], have not been interpreted as incomplete ionization.

How does our parametrization compare with experimental data at lower temperatures, where i.i. is significantly stronger? We compare it in Fig. 7 with Hall measurements[137] between $T=30$ and 180 K. In these measurements, $r=1$ was assumed. We do not know the precise value of r under these conditions.[26,125,127] Measurements indicate that it decreases[129,130,138] (or increases[139,140]) with decreasing T at $N_{dop}\lesssim N_{crit}$ (or at $N_{dop}\gtrsim N_{crit}$). This is the reason why the measured values at $N_{dop}=4.2\times10^{18}$ cm^{-3} in Fig. 7 increase slightly with decreasing T. Within these uncertainties, our parametrization agrees with the measurements and describes i.i. also at low temperatures reasonably well.

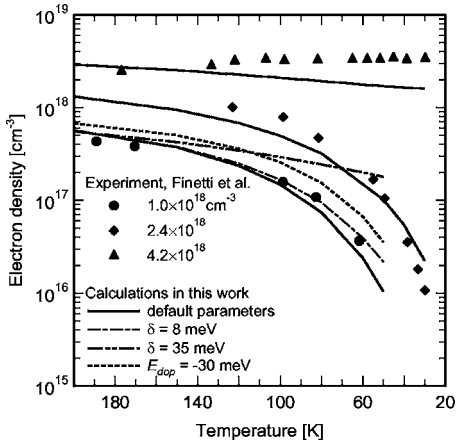

FIG. 7. The density of free electrons, derived from Hall measurements (Ref. 137) (symbols), compared to the parametrization of Eqs. (10a)–(10c) (solid lines). The dashed lines are calculated at $N_{dop}=1\times10^{18}$ cm^{-3}, using $\delta=9$ and 35 meV, respectively (instead of 2.8 meV), or $E_{dop}=-30$ meV (instead of −40.95 meV).

In Sec. III, the fitting parameters were adjusted at 4.2 K and changes at higher temperatures were neglected. Therefore, the solid lines in Fig. 7 are calculated at all temperatures with E_{dop} and δ obtained at 4.2 K. To test whether this is a useful approach, E_{dop} and δ are now varied at $N_{dop}=1\times10^{18}$ cm^{-3}, shown as dashed lines in Fig. 7. The following two features become apparent: Firstly, when E_{dop} is reduced by 30% from the value given at 4.2 K, the predicted n values are too high at $T<200$ K. Apparently, E_{dop} depends only very weakly on T, as is expected from the nonlinear Thomas-Fermi-Dirac screening theory.[13] Secondly, we mentioned in Sec. IV that temperature effects may broaden the dopant band. For example, if $\delta=9$ meV (or $\delta=35$ meV) is used instead of $\delta=2.8$ meV, n stays compatible with the measurements at $T>50$ K (or $T>150$ K). This very large broadening does not influence n significantly because it is symmetrical with respect to E_{dop}. These two tests demonstrate that our approximation of a temperature-independent DOS is indeed useful.

VI. CONCLUSIONS

Reinterpreting photoluminescence and tunneling measurements, it was shown that the phosphorus dopant band only "touches" the conduction band at the Mott (metal-insulator) transition and that it merges with the conduction band at considerably higher dopant densities ($N_{dop}\approx2\times10^{19}$ cm^{-3}). This resolves well-known contradictions between photoconductivity, infrared absorption, dielectric, magnetic resonance, infrared reflectance, and specific heat measurements. Based on a thorough collection and reinterpretation of published measurements, it was verified that at room temperature, up to 25% of dopants are nonionized near $N_{dop}\approx2\times10^{18}$ cm^{-3}. This is contrary to common assumptions that incomplete ionization can be neglected at room temperature. It was demonstrated that there exists no significant amount of incomplete ionization far above the Mott transition ($N_{dop}>2\times10^{19}$ cm^{-3}).

ACKNOWLEDGMENTS

One of the authors (P.P.A.) conducted part of this research while he was supported by a Queen Elizabeth II Fellowship from the Australian Research Council (ARC) at the Australian National University in Canberra, Australia, as a visiting Senior Researcher at the School of Computer Science and Engineering, University of NSW, Sydney, and as an ARC Postdoctoral Researcher at the Photovoltaics Research Centre at UNSW.

APPENDIX A

We claimed in Sec. II B that the measurements of Refs. 36–39 determine E_{act} and not E_{dop}, as originally thought. We justify our claim as follows. Reference 36 extracted the data from photoconductivity measurements performed at 4.2 K. The photon energies taken for the extraction of E_{dop} excited the electrons from the highest occupied dopant states to the lowest states in the conduction band. We argue that E_{act} was measured, because the dopant band is practically completely occupied at such low temperatures (this is also supported by

electron paramagnetic resonance studies[122] and Seebeck measurements[78]). Reference 37 measured the conductivity of silicon at $T<10$ K. Applying the same arguments again, we conclude that in such measurements, the electrons in the highest dopant states were thermally excited to the conduction band in order to contribute to the dc conductivity. Hence, these measurements yielded E_{act}. Similar arguments apply again to the infrared absorption measurements of Ref. 38. The data of Ref. 39, obtained at 2 K, are derived from the dielectric constant in Ref. 42, using a procedure described in Ref. 141. It is argued in Ref. 42 that such measurements yield E_{act}.

APPENDIX B

We reevaluated the DOS data of Nishizawa and Kimura,[70] shown in Fig. 1(e). Originally, these authors evaluated their I-V data without taking the broadening of the dopant band into account.[70] For example, they extracted E_{Fn} from the minimum of the measured (dI/dV)-V curve. However, later investigations[64] demonstrated that this minimum is shifted by approximately 10 meV due to the dopant band. Thus, we shifted the DOS data of Nishizawa and Kimura by 11 meV to lower energies. Without this shift, their original DOS data would be inconsistent with the PL measurements at both high and low injection levels. Nishizawa and Kimura had to adjust the effective electron mass at a higher value than is generally accepted, because they needed to compensate for effects occurring from their assumption that E_{Fn} is situated above the conduction band edge at $N_{dop}<1\times10^{19}$ cm^{-3}. However, magnetic resonance measurements[40] indicate that, near the M-I transition, the Fermi level has not reached the conduction band.

[1] H. Watanabe and S. Takagi, J. Appl. Phys. **90**, 1600 (2001).
[2] G. Xiao, J. Lee, J. J. Liou, and A. Ortiz-Conde, Microelectron. Reliab. **39**, 1299 (1999).
[3] Y. T. Lee, D. S. Woo, J. D. Lee, and B. G. Park, J. Korean Phys. Soc. **33**, S200 (1998).
[4] Y. Yue and J. J. Liou, Solid-State Electron. **39**, 318 (1996).
[5] G. L. Pearson and J. Bardeen, Phys. Rev. **75**, 865 (1949).
[6] R. A. Abram, G. J. Rees, and B. L. H. Wilson, Adv. Phys. **27**, 799 (1978).
[7] P. A. Lee and T. V. Ramakrishnan, Rev. Mod. Phys. **57**, 287 (1985).
[8] D. Belitz and T. R. Kirkpatrick, Rev. Mod. Phys. **66**, 261 (1994).
[9] R. G. Aggarwal and A. K. Ramdas, Phys. Rev. **140**, A1246 (1965).
[10] D. Karaiskaj, T. A. Meyer, M. L. W. Thewalt, and M. Cordona, Phys. Rev. B **68**, 121201 (2003).
[11] R. G. Pires, R. M. Dickstein, S. L. Titcomb, and R. L. Anderson, Cryogenics **30**, 1064 (1990).
[12] F. Bassani, G. Iadonisi, and B. Preziosi, Rep. Prog. Phys. **37**, 1099 (1974).
[13] Y. P. Varshni and S. M. Khanna, Phys. Rev. B **43**, 9279 (1991).
[14] A. L. Efros, Sov. Phys. Usp. **16**, 789 (1974).
[15] L. V. Keldysh and G. P. Proshko, Sov. Phys. Solid State **5**, 2481 (1964).
[16] E. O. Kane, Solid-State Electron. **28**, 3 (1985).
[17] G. A. Thomas, M. Capizzi, F. DeRosa, R. N. Bhatt, and T. M. Rice, Phys. Rev. B **23**, 5472 (1981).
[18] D. Karaiskaj, J. A. H. Stotz, T. Meyer, M. L. W. Thewalt, and M. Cardona, Phys. Rev. Lett. **90**, 186402 (2003).
[19] D. F. Holcomb and J. J. Rehr, Phys. Rev. **183**, 773 (1969).
[20] R. Riklund and K. A. Chao, Phys. Rev. B **26**, 2168 (1982).
[21] D. New and T. G. Castner, Phys. Rev. B **29**, 2077 (1984).
[22] D. New, Phys. Rev. B **32**, 2419 (1985).
[23] A. Roy, M. Turner, and M. P. Sarachik, Phys. Rev. B **37**, 5522 (1988).
[24] M. Lakner, H. v. Löhneysen, A. Langenfeld, and P. Wölfle, Phys. Rev. B **50**, 17064 (1994).
[25] R. N. Bhatt and T. M. Rice, Philos. Mag. B **42**, 859 (1980).
[26] J. D. Quirt and J. R. Marko, Phys. Rev. B **7**, 3842 (1973).
[27] N. Mikoshiba, Rev. Mod. Phys. **40**, 833 (1968).
[28] J. R. Marko, J. P. Harrison, and J. D. Quirt, Phys. Rev. B **10**, 2448 (1974).
[29] V. Radhakrishnan, P. C. Sharma, and M. Singh, Z. Phys. B: Condens. Matter **39**, 15 (1980).
[30] T. F. Rosenbaum, R. F. Milligan, M. A. Paalanen, G. A. Thomas, R. N. Bhatt, and W. Lin, Phys. Rev. B **27**, 7509 (1983).
[31] A. Blaschette, A. Ruzzu, S. Wagner, and H. v. Löhneysen, Europhys. Lett. **36**, 527 (1996).
[32] S. Kobayashi, Y. Monden, and W. Sasaki, Solid State Commun. **30**, 661 (1979).
[33] F. Mousty, P. Ostoja, and L. Passari, J. Appl. Phys. **45**, 4576 (1974).
[34] W. R. Thurber, R. L. Mattis, Y. M. Liu, and J. J. Filiben, J. Electrochem. Soc. **127**, 1807 (1980).
[35] W. Baltensperger, Philos. Mag. **44**, 1355 (1953).
[36] G. M. Guichar, C. Sebenne, F. Proix, and M. Balkanski, Phys. Rev. B **5**, 422 (1972).
[37] S. Toyotomi, J. Phys. Soc. Jpn. **38**, 175 (1975).
[38] W. Scott and C. E. Jones, J. Appl. Phys. **50**, 7258 (1979).
[39] M. Capizzi, G. A. Thomas, F. D. Rosa, R. N. Bhatt, and T. M. Rice, Phys. Rev. Lett. **44**, 1019 (1980).
[40] D. Jerome, C. Ryter, H. J. Schulz, and J. Friedel, Philos. Mag. B **52**, 403 (1985).
[41] A. Gaymann, H. P. Geserich, and H. v. Löhneysen, Phys. Rev. Lett. **71**, 3681 (1993).
[42] R. N. Bhatt and T. M. Rice, Phys. Rev. B **23**, 1920 (1981).
[43] B. Bergersen, J. A. Rostworowski, M. Eswaran, R. R. Parsons, and P. Jena, Phys. Rev. B **14**, 1633 (1976).
[44] M. Eswaran, B. Bergersen, J. A. Rostworowski, and R. R. Parsons, Solid State Commun. **20**, 811 (1976).
[45] R. R. Parsons, Solid State Commun. **29**, 1 (1979).
[46] O. J. Glembocki and F. H. Pollak, Phys. Rev. B **25**, 1193 (1982).
[47] M. Asche and O. Sarbei, Phys. Status Solidi B **103**, 11 (1981).
[48] R. Pässler, Solid-State Electron. **39**, 1311 (1996).
[49] A. Schenk, J. Appl. Phys. **84**, 3684 (1998).
[50] Bergersen *et al.*, presumed an electron-hole droplet to exist, but this was revoked after successive studies (Ref. 45) For the reinterpretation of the PL data, we do not need to introduce an electron-hole droplet either (Ref. 49) to come to a coherent solution.
[51] C. Benoit à la Guillaume and M. Voos, Phys. Rev. B **7**, 1723 (1973).
[52] P. T. Landsberg and D. J. Robbins, Solid-State Electron. **28**, 137 (1985).
[53] M. L. W. Thewalt, G. Kirczenow, R. R. Parsons, and R. Barrie, Can. J. Phys. **54**, 1728 (1976).
[54] J. Menendez and M. Cardona, Phys. Rev. B **29**, 2051 (1984).
[55] F. Cerdeira, T. A. Fjeldly, and M. Cardona, Phys. Rev. B **8**, 4734 (1973).
[56] L. Pintschovius, J. A. Vergés, and M. Cardona, Phys. Rev. B **26**, 5658 (1982).
[57] J. Shah, M. Combescot, and A. H. Dayem, Phys. Rev. Lett. **38**, 1497 (1977).
[58] J. Monecke, J. Kortus, and W. Cordts, Phys. Rev. B **47**, 9377 (1993).
[59] W. D. Straub, H. Roth, W. Bernard, S. Goldstein, and J. E. Mulhern, Phys. Rev. Lett. **21**, 752 (1968).
[60] M. Lakner and H. v. Löhneysen, Phys. Rev. Lett. **70**, 3475 (1993).
[61] V. Dyakonov and G. Denninger, Phys. Rev. B **46**, 5008 (1992).
[62] J. Serre and A. Ghazali, Phys. Rev. B **28**, 4704 (1983).
[63] A. Ghazali and J. Serre, Solid-State Electron. **28**, 145 (1985).
[64] K. P. Abdurakhmanov, S. Mirakhmedov, and A. T. Teshabaev, Sov. Phys. Semicond. **12**, 457 (1987).
[65] G. D. Mahan and J. W. Conley, Appl. Phys. Lett. **11**, 29 (1967).
[66] J. W. Conley and G. D. Mahan, Phys. Rev. **161**, 681 (1967).
[67] K. P. Abdurakhmanov, S. Mirakhmedov, A. Teshabaev, and S. S. Khudaiberdiev, Sov. Phys. Semicond. **10**, 393 (1976).
[68] H. G. Busmann, S. Ewert, W. Sander, K. Seibert, P. Balk, and A. Steffen, Z. Phys. B: Condens. Matter **59**, 439 (1985).
[69] G. Salace and J. M. Patat, Thin Solid Films **207**, 213 (1992).
[70] J. Nishizawa and M. Kimura, Jpn. J. Appl. Phys. **14**, 1529 (1975).
[71] M. N. Alexander and D. F. Holcomb, Rev. Mod. Phys. **40**, 815 (1968).
[72] K. F. Berggren and B. E. Sernelius, Phys. Rev. B **24**, 1971 (1981).
[73] R. E. Halliwell and R. R. Parsons, Can. J. Phys. **52**, 1336 (1974).
[74] J. Wagner, Phys. Rev. B **29**, 2002 (1984).
[75] N. Kobayashi, S. Ikehata, S. Kobayashi, and W. Sasaki, Solid State Commun. **32**, 1147 (1979).
[76] N. Kobayashi, S. Ikehata, S. Kobayashi, and W. Sasaki, Solid State Commun. **24**, 67 (1977).

[77]R. K. Sundfors and D. F. Holcomb, Phys. Rev. **136**, A810 (1964).
[78]T. Geballe and G. W. Hull, Phys. Rev. **98**, 940 (1955).
[79]R. Keyes, Solid State Commun. **32**, 179 (1979).
[80]M. Miyao, T. Motooka, N. Natsuaki, and T. Tokuyama, Solid State Commun. **37**, 605 (1981).
[81]A. Schenk, J. Appl. Phys. **79**, 814 (1996).
[82]A. Selloni and S. T. Pantelides, Phys. Rev. Lett. **49**, 586 (1982).
[83]E. O. Kane, Phys. Rev. **131**, 79 (1963).
[84]J. C. Phillips, Europhys. Lett. **14**, 367 (1991).
[85]E. Daub and P. Würfel, J. Appl. Phys. **80**, 5325 (1996).
[86]S. M. Sze, *Physics of Semiconductor Devices*, 2nd ed. (Wiley, New York, 1981).
[87]U. Pietsch and K. Unger, Phys. Status Solidi A **80**, 165 (1983).
[88]I. Yokota, J. Phys. Soc. Jpn. **19**, 1487 (1964).
[89]M. A. Green, J. Appl. Phys. **67**, 2944 (1990).
[90]T. N. Morgan, Phys. Rev. **139**, A343 (1965).
[91]A. Lü, Z. Zhang, K. A. Chao, and J. Zhu, Phys. Rev. B **31**, 8087 (1985).
[92]K. L. Liu, B. Bergersen, and P. Modrak, Can. J. Phys. **58**, 1142 (1980).
[93]K. L. Liu, P. Modrak, and B. Bergersen, Can. J. Phys. **60**, 1743 (1982).
[94]K. L. Liu and B. Bergersen, Can. J. Phys. **59**, 141 (1981).
[95]K. Morigaki and F. Yonezawa, Prog. Theor. Phys. **57**, 146 (1975).
[96]S. Sumerfield, J. A. McInnes, and P. N. Butcher, J. Phys. C **20**, 3647 (1987).
[97]W. C. de Oliveira and E. V. Anda, Solid State Commun. **69**, 575 (1989).
[98]R. M. Swanson and S. E. Swirhun, Sandia National Laboratories Technical Report No. SAND97–7019, 1987.
[99]N. A. Penin, B. G. Zhurkin, and B. A. Volkov, Sov. Phys. Solid State **7**, 2580 (1966).
[100]M. Levy, P. Y. Yu, Y. Zhang, and M. P. Sarachik, Phys. Rev. B **49**, 1677 (1994).
[101]Y. Nishio, K. Kajita, and W. Sasaki, Solid State Commun. **79**, 1017 (1991).
[102]U. Thomanschefsky and D. F. Holcomb, Phys. Rev. B **45**, 13356 (1992).
[103]M. J. Hirsch, D. F. Holcomb, R. N. Bhatt, and M. A. Paalanen, Phys. Rev. Lett. **68**, 1418 (1992).
[104]J. Serre, A. Ghazali, and P. Leuroux Hgon, Phys. Rev. B **23**, 1971 (1981).
[105]A. P. Levanyuk and V. V. Osipov, Sov. Phys. Semicond. **7**, 721 (1973).
[106]A. P. Levanyuk and V. V. Osipov, Sov. Phys. Semicond. **7**, 727 (1973).
[107]T. G. Castner, Phys. Rev. B **21**, 3523 (1980).
[108]S. S. Li, *The Dopant Density and Temperature Dependence of Electron Mobility and Resistivity in n-Type Silicon*, Nat. Bur. Stand. (U.S.) Spec. Publ. No. 400–33 (U.S. GPO, Washington, DC, 1977).
[109]S. S. Li and W. R. Thurber, Solid-State Electron. **20**, 609 (1977).
[110]T. F. Lee and T. C. McGill, J. Appl. Phys. **46**, 373 (1975).
[111]J. R. Lowney, A. H. Kahn, J. L. Blue, and C. L. Wilson, J. Appl. Phys. **52**, 4075 (1981).
[112]J. Hubbard, Proc. R. Soc. London, Ser. A **281**, 401 (1964).
[113]N. F. Mott and J. H. Davies, Philos. Mag. B **42**, 845 (1980).
[114]M. Taniguchi and S. Narita, Solid State Commun. **20**, 131 (1976).
[115]P. Norton, J. Appl. Phys. **47**, 308 (1976).
[116]P. Norton, Phys. Rev. Lett. **37**, 164 (1976).
[117]J. Wagner and J. A. del Alamo, J. Appl. Phys. **63**, 425 (1988).
[118]J. Wagner, Phys. Rev. B **32**, 1323 (1985).
[119]R. R. Parsons, Can. J. Phys. **56**, 814 (1978).
[120]R. R. Parsons, Solid State Commun. **29**, 763 (1979).
[121]R. R. Parsons, J. A. Rostworowski, R. E. Halliwell, and R. Barrie, Can. J. Phys. **55**, 1349 (1977).
[122]J. D. Quirt and J. R. Marko, Phys. Rev. B **5**, 1716 (1972).
[123]P. Landsberg, Proc. Phys. Soc., London, Sect. A **65**, 604 (1952).
[124]E. A. Guggenheim, Proc. Phys. Soc., London, Sect. A **66**, 121 (1953).
[125]P. Norton, T. Braggins, and H. Levinstein, Phys. Rev. B **8**, 5632 (1973).
[126]W. R. Thurber, J. Electron. Mater. **9**, 551 (1980).
[127]J. A. del Alamo and R. M. Swanson, J. Appl. Phys. **57**, 2314 (1985).
[128]W. R. Thurber, R. L. Mattis, Y. M. Liu, and J. J. Filliben, *The Relationship Between Resistivity and Dopant Density for Phosphorous- and Boron-Doped Silicon*, Natl. Bur. Stand. (U.S.) Spec. Publ. No. 400–64 (U.S. GPO, Washington, DC, 1981).
[129]D. Long, Phys. Rev. **120**, 2024 (1960).
[130]J. Messier and J. M. Flores, J. Phys. Chem. Solids **24**, 1539 (1963).
[131]L. Esaki and Y. Miyahara, Solid-State Electron. **1**, 13 (1960).
[132]P. G. Litovchenko, V. S. Lutsyak, I. G. Kirnas, P. M. Kurilo, and V. M. Nitsovich, Phys. Status Solidi A **21**, 419 (1974).
[133]S. Nakanuma, J. Electrochem. Soc. **111**, 1199 (1964).
[134]P. Altermatt, G. Heiser, and A. Schenk (unpublished).
[135]W. Kuzmicz, Solid-State Electron. **29**, 1223 (1986).
[136]W. Nuyts and R. van Overstraeten, J. Appl. Phys. **42**, 3988 (1971).
[137]M. Finetti, A. M. Mazzone, L. Passari, S. Pietra, and E. Susi, J. Appl. Phys. **47**, 4590 (1976).
[138]F. J. Morin and J. P. Maita, Phys. Rev. **96**, 28 (1954).
[139]C. Yamanouchi, K. Mizuguchi, and W. Sasaki, J. Phys. Soc. Jpn. **22**, 859 (1967).
[140]N. N. Dmitrenko, I. G. Kirnas, P. M. Kurilo, P. G. Litovchenko, V. S. Lutsyak, and V. M. Nitsovitch, Phys. Status Solidi A **26**, K45 (1974).
[141]P. L. Hugon and A. Ghazali, Phys. Rev. B **14**, 602 (1976).